
COXSE: EXPLORING THE POTENTIAL OF SELF-EXPLAINING NEURAL NETWORKS WITH COX PROPORTIONAL HAZARDS MODEL FOR SURVIVAL ANALYSIS

Abdallah Alabdallah¹, Omar Hamed¹, Mattias Ohlsson^{1,3}, Thorsteinn Rögnavaldsson¹, and Sepideh Pashami^{1,2}

¹Center for Applied Intelligent Systems Research (CAISR), Halmstad University
Halmstad, Sweden

²Research Institutes of Sweden (RISE)
Stockholm, Sweden

³Dept. Astronomy and Theoretical Physics, Lund University
Lund, Sweden

July 22, 2024

ABSTRACT

The Cox Proportional Hazards (CPH) model has long been the preferred survival model for its explainability. However, to increase its predictive power beyond its linear log-risk, it was extended to utilize deep neural networks sacrificing its explainability. In this work, we explore the potential of self-explaining neural networks (SENN) for survival analysis. We propose a new locally explainable Cox proportional hazards model, named CoxSE, by estimating a locally-linear log-hazard function using the SENN. We also propose a modification to the Neural additive (NAM) models hybrid with SENN, named CoxSENAM, which enables the control of the stability and consistency of the generated explanations.

Several experiments using synthetic and real datasets have been performed comparing with a NAM-based model, DeepSurv model explained with SHAP, and a linear CPH model. The results show that, unlike the NAM-based model, the SENN-based model can provide more stable and consistent explanations while maintaining the same expressiveness power of the black-box model. The results also show that, due to their structural design, NAM-based models demonstrated better robustness to non-informative features. Among these models, the hybrid model exhibited the best robustness.

Keywords Self-Explaining Neural Networks · Cox Proportional Hazards · Survival Analysis · Interpretability · XAI · Neural Additive Models

1 Introduction

Due to their flexibility and the abundance of collected data, neural-network-based models have been shown to outperform classical machine learning methods in survival modeling [1]. However, such performance gain comes at the price of their explainability. Neural networks have long been considered black-box models because of their complicated inner workings. This makes it difficult to understand how they arrive at their predictions. This hinders the usability of such models especially in domains like survival analysis when used for safety-critical applications like some areas in health care or predictive maintenance [2, 3, 4, 5]. Nonetheless, efforts have been spent utilizing post-hoc explanation methods to compensate for the lack of transparency in black-box models [6].

Recently, there has been a growing interest in a type of neural network that not only predicts the outcome of an instance but also provides inherent explanations of how it arrived at such an outcome. Examples of such an approach are the Neural Additive Models (NAM) [7] and the Self-Explaining Neural Networks (SENN) [8]. Such models can learn to fit the problem while providing intrinsic explanations for their decisions. The NAM method converts the problem into a

sum of single-input functions of individual features. Each single-input function is modeled as a neural network, the output of which represents the respective feature’s contribution to the decision. On the other hand, SENN models the function as locally-linear function where the model learns the relevance of the features conditioned on the input.

The NAM structure was first used for survival analysis in SurvNAM [9] as a surrogate Cox-based model to explain black-box survival models. Subsequently, it was recently proposed as a stand-alone model named CoxNAM [10]. However, due to its structural design, the NAM models cannot model feature interactions limiting their predictive power. Moreover, the NAM models provide explanations that highlight the contribution of each feature to the decision omitting the model’s sensitivity to change in those features.

Therefore, in this work, we explore the potential of the SENN structure for survival modeling. We propose CoxSE, a Cox-based self-explaining model relying on the SENN structure. CoxSE learns features’ relevance which can be interpreted as the weights of the line tangent to the decision boundary in the vicinity of the point of interest. As all features contribute to the computation of each feature’s relevance, CoxSE can account for feature interactions. Additionally, CoxSE has two extra regularization terms to encourage the stability and consistency of the provided explanations.

However, such flexibility comes with a price, as the NAM structure is shown to be more robust to noise. Therefore, we also propose a hybrid model CoxSENAM, adopting the NAM structure and the type of output of the SENN along with its loss function’s regularization terms. Similar to CoxNAM, such a model is more suitable for cases with no feature interactions, however, it benefits from the extra regularization of the learned features’ relevance, achieving better stability, consistency, and robustness.

2 Survival Analysis

Survival analysis is a branch of statistics concerned with studying the time until an event of interest occurs, for example, a patient’s death or a machine’s failure. The main challenge that gave rise to such a branch of science is that the collected data contains subjects that have not experienced the event yet at the end of the study. Such cases are called censored cases which are assumed to experience the event at a later time greater than their recorded time, in which case it is called right censored data. There are other types of censoring, however, right censoring is the most common.

Survival data usually comes as tuples of three variables (\mathbf{x}_i, t_i, e_i) that describe, for each subject (i) , the features’ vector \mathbf{x}_i , the recorded time t_i , and the event indicator e_i to indicate whether the recorded time is the time-to-event or the censoring time.

The survival and hazard functions are the two main functions that survival analysis usually endeavors to estimate. Given survival time as a random variable T , the survival function is defined as the probability of survival beyond time t :

$$S(t) = P(T > t) \quad (1)$$

The hazard function represents the instantaneous death rate which quantifies the risk of the event in the infinitesimal time δt given that the subject has survived until the time t and is defined as:

$$h(t) = \lim_{\Delta t \rightarrow 0} \frac{P(t \leq T < t + \Delta t | T \geq t)}{\Delta t} \quad (2)$$

Those two functions are related where:

$$h(t) = -\frac{d}{dt} \ln(S(t)) \quad (3)$$

The cumulative hazard function (CHF) is another function of interest to some models and is related to the hazard and survival functions:

$$H(t) = \int_0^t h(\tau) d\tau \quad (4)$$

and:

$$S(t) = e^{-H(t)} \quad (5)$$

Early on, statistical methods have been developed to estimate such functions as the Kaplan-Meier estimator [11] to estimate the survival function or the Nelson-Aalen estimator [12, 13, 14] to estimate the CHF. However, the Cox Proportional Hazards Model (CPH) [15] is the first model to account for feature dependency. The CPH model assumes a baseline hazard function $h_0(t)$ common to all subjects and only depends on time. Whereas, the features \mathbf{x} have exponential multiplicative effects on the hazard that is independent of time. As a result, there is a linear relationship between the features and the logarithm of the hazard function:

$$h(t, \mathbf{x}) = h_0(t) e^{\mathbf{w}^T \mathbf{x}} \quad (6)$$

Due to its linearity, the CPH model is considered to be explainable, where the weights \mathbf{w} indicate the relative importance of the features in the decision.

Subsequently, machine learning started to be used for survival analysis, offering more accurate and flexible models. Also, more recently, with the abundance of collected data, deep learning models in particular emerged as the predominant approach. Numerous deep-learning models have been proposed to estimate different survival analysis functions employing various techniques and objective functions for this purpose [16, 17, 1, 18]. Interestingly, over 40% of such models employ the Cox-based formulation [19]. Most notably DeepSurv [16] which extends the CPH linear log-risk function ($\mathbf{w}^\top \mathbf{x}$ in Equation 6) to a non-linear function ($f(x)$ in Equation 7) modeled as a neural network.

$$h(t, \mathbf{x}) = h_0(t)e^{f(\mathbf{x})} \quad (7)$$

There are many evaluation metrics used to evaluate survival models. However, the concordance index (C-index) [20] is arguably the most frequently used metric. The C-index quantifies the rank correlation between the predicted scores of subjects and their observed or censored times. More specifically, it represents the probability that the predicted risk scores of two randomly selected subjects agree with the order of their observed event times as stated in Equation 8. Thus, a good model should assign higher risk scores for subjects with shorter survival times leading to a higher C-index value.

$$CI = \mathbb{P}(\hat{r}_i > \hat{r}_j | t_i < t_j, e_i = 1) \quad (8)$$

where \hat{r}_i is the predicted risk score of the subject i with the time-to-event value t_i and event indicator e_i .

The concordance index is closely related to the CPH model in the sense that both focus on the rank order of events and are insensitive to any monotonic transformation. Such a relation makes the C-index suitable for our purpose as all the models in this work follow the assumptions of the Cox Proportional Hazards model.

3 Related work

As machine learning started to be used for survival analysis, a need for suitable explainability methods emerged—survival models usually output functions, which hinders the use of machine learning explanation methods. Many post-hoc explanation methods in machine learning like LIME [21] and SHAP [22] have been adapted to survival analysis models as in [23, 24, 25]. Moreover, other methods relied on counterfactual examples adapting them for survival models [26, 27].

However, a growing direction focuses on building inherently explainable, yet expressive, models. SurvNAM [9] proposed the use of Neural Additive Models (NAM) [7] and an extended Cox-Proportional Hazards model as a surrogate model to explain black-box survival models. More recently, CoxNAM [10] proposed using the NAM structure with the Cox formulation as a standalone inherently explainable survival model.

Originally, the NAM models the relation between an input $\mathbf{x} = (x_0, x_1, \dots, x_p)$ and a target y as an additive function based on the Generalized Additive Models (GAM) model [28]:

$$\mathbb{E}(y) = \sum_{i=0}^p g_i(x_i) \quad (9)$$

where in the NAM model, the g_i functions are modeled as neural networks.

The CoxNAM model uses the same scheme, however, to model the hazard function based on the Cox Proportional Hazards formulation as illustrated in Figure 1. Due to their design, NAM-based models cannot model interactions between features. This limits the expressive power of such models leading to underfitting in most cases. Moreover, there is no guarantee that the model will learn valid explanations.

Our work relies on another interesting direction for inherent explanations, the Self-Explaining Neural Networks (SENN) [8]. Such a model has two branches: a concept encoder that generates interpretable features $h(\mathbf{x})$ from the input and an input-dependent parameterizer that learns the features' relevance scores (weights) $\mathbf{w}(\mathbf{x})$. Eventually, the function can be written as:

$$f(x) = g(w_1(\mathbf{x})h_1(\mathbf{x}), \dots, w_p(\mathbf{x})h_p(\mathbf{x})) \quad (10)$$

where $g(\cdot)$ is the aggregation function and can be any affine function with positive weights or simply an addition. For tabular data, the concept vector is the original feature space, i.e. $h(\mathbf{x}) = \mathbf{x}$, approximating the function with a locally-linear function. Additionally, SENNs regularize their generated explanations to ensure that similar subjects have similar explanations, a quality referred to as stability.

As the weights of each feature depend on all the features, SENN can model the interactions between the features maintaining similar performance as regular neural networks. Moreover, SENN with its regularization can control the quality of the explanations.

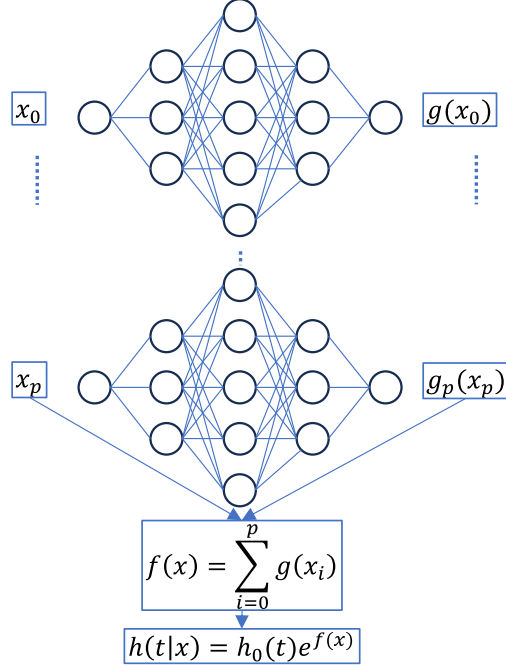


Figure 1: CoxNAM Model architecture

4 Method

Our method CoxSE extends the self-explaining neural network (SENN) [8] to survival analysis using the Cox Proportional Hazards model (CPH) [15], however, with non-linear relationship $f(\mathbf{x})$ between the predictors and the hazard as shown in Equation 11:

$$h(t, \mathbf{x}) = h_0(t)e^{f(\mathbf{x})} \quad (11)$$

where $h_0(t)$ is an unspecified baseline hazard function and the log-risk function $f(\mathbf{x})$ is approximated as a locally linear function:

$$f(\mathbf{x}) = \sum_{x_i \in \mathbf{x}} w_{\theta_i}(\mathbf{x})x_i \quad (12)$$

This allows the model to learn the relevance vector $\mathbf{w}_{\theta}(\mathbf{x})$ that specifies the linear weights at each point \mathbf{x} . Such weights describe a vector perpendicular to the decision boundary and reflect the local features' importance at each specific location. An illustration of the CoxSE model is shown in Figure 2.

Based on the SENN and the NAM models we also propose a hybrid mode named CoxSENAM. As illustrated in Figure 3, the model has a structure similar to the CoxNAM model and a type of output and loss function similar to the CoxSE model. In this model, features' relevance are computed independently:

$$f(\mathbf{x}) = \sum_{x_i \in \mathbf{x}} w_{\theta_i}(x_i)x_i \quad (13)$$

where w_{θ_i} is the relevance function of the i 'th feature in the features' vector \mathbf{x} .

The loss function consists of three terms. The first term is the Partial Likelihood function inherited from the CPH model, Equation 14. This part of the loss function maximizes the concordance between the predicted hazards.

$$\mathcal{L}_1(\theta) = \prod_{i=1}^N \frac{e^{f_{\theta}(\mathbf{x}_i)}}{\sum_{\mathbf{x}_j \in R_i} e^{f_{\theta}(\mathbf{x}_j)}} \quad (14)$$

where R_i are the subjects at risk at time t_i .

The second term, Equation 15, minimizes the distance between $\nabla_x f_{\theta}(\mathbf{x})$, the gradient of $f_{\theta}(\mathbf{x})$ with respect to \mathbf{x} , and the predicted local weights $w_{\theta}(\mathbf{x})$:

$$\mathcal{L}_2(\theta) = \|\nabla_x f_{\theta}(\mathbf{x}) - w_{\theta}(\mathbf{x})\|_2 \quad (15)$$

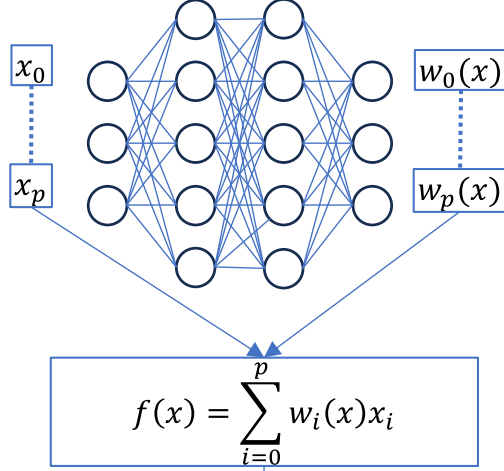


Figure 2: CoxSE Model architecture

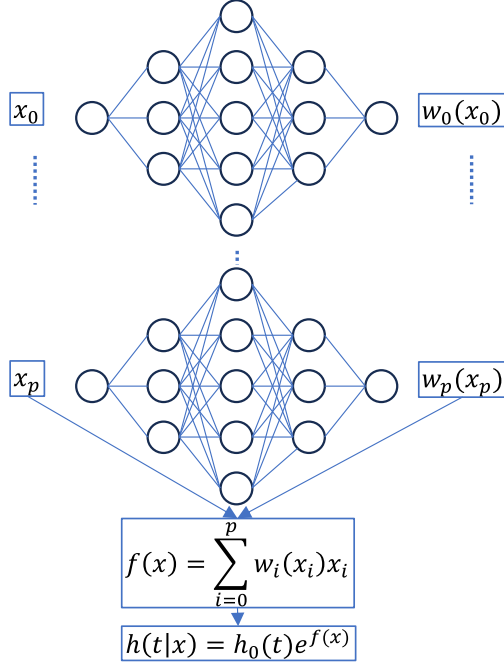


Figure 3: CoxSENAM Model architecture

This term is adopted from the SENN model to encourage explanations’ stability. We also added a third term to the loss function that regularizes the learned weights and encourages the model to select a subset of the most important features while setting the weights of less important features to zero:

$$\mathcal{L}_3(\theta) = \|w_\theta(\mathbf{x})\|_1 \tag{16}$$

The three terms comprise the loss function:

$$\mathcal{L}(\theta) = \mathcal{L}_1(\theta) + \alpha\mathcal{L}_2(\theta) + \beta\mathcal{L}_3(\theta) \tag{17}$$

4.1 Datasets

Three synthetic datasets are created with different characteristics following the proportional hazards assumption. Moreover, two real datasets were used in the experiments.

4.1.1 Lin Dataset

A synthetic dataset that consists of 50000 subjects with three features of increasing importance, and a linear relationship between the log-risk $f(\mathbf{x})$ and the predictors as follows:

$$f(\mathbf{x}) = 0.44x_0 + 0.66x_1 + 0.88x_2 \quad (18)$$

4.1.2 NonLin Dataset

A synthetic dataset that consists of 50000 subjects with three features and a non-linear relationship between the log-risk $f(\mathbf{x})$ and the predictors and different importance represented by the feature weights as follows:

$$f(\mathbf{x}) = 3x_0^2 + 2x_1^2 + x_2^2 \quad (19)$$

4.1.3 NonLinX Dataset

A synthetic dataset that consists of 50000 subjects with three features and a non-linear relationship between the log-risk $f(\mathbf{x})$ and the predictors, different importance represented by the feature weights, and an interaction between the first two features, as follows:

$$f(\mathbf{x}) = 3x_0^2 + 2x_1^2 + x_2^2 + 3x_0x_1 \quad (20)$$

4.1.4 FLCHAIN Dataset

This survival analysis benchmark dataset is used to study whether the free light chain (FLC) assay is a good predictor of survival time [29]. The dataset consists of 7874 subjects with 27 numerical and one-hot-encoded features, where the FLC is the sum of the two features kappa and lambda. As a result, the study found that a high FLC value was a significant predictor of worse survival.

4.1.5 SEER Dataset

The Surveillance, Epidemiology, and End Results (SEER) database [30], maintained by the US National Cancer Institute, is a comprehensive dataset that gathers detailed information on cancer patients. This dataset includes data on diagnoses, treatments, and survival rates. We utilized version 8.4.3 of the "SEER*Stat" software and the "Incidence – SEER research data, 17 registries" release from November 2022. The dataset encompasses cancer incidences from 2000 to 2020. However, we narrowed our analysis to incidences between 2004 and 2015 to avoid preprocessing challenges due to different coding systems used across various years. The dataset consists of 458117 subjects with 32 numerical, label-encoded, and one-hot-encoded features.

5 Experiments

5.1 Experiment Settings

Five models, all based on Cox Proportional Hazards are compared, CPH, DeepSurv, CoxNAM, CoxSE, and CoxSENAM. All those models are self-explaining except for DeepSurv for which the SHAP method is used to explain. Experiments on the three synthetic and the two real datasets were conducted. Five-fold cross-validation is used to tune the neural networks' hyperparameters, Number of Layers, Number of Nodes, L2 regularization, Dropout, and Learning rate. In addition to α and β , the weights of the CoxSE and CoxSENAM loss function. More details about the hyperparameters are available in A.

5.2 Models Performance

Results in Table 1 show that all models performed similarly on the Lin dataset. Also, the four deep-learning-based models performed similarly on the NonLin dataset except for the CPH model, which could not model the non-linear relationship in the data. The more remarkable case is the NonLinX, the non-linear synthetic dataset with interactions between the features. On this dataset, both, DeepSurv and CoxSE performed similarly. However, CoxNAM and CoxSENAM failed to model the feature interaction and converged to a significantly lower C-index. In this case, CPH also failed to model the data and converged to a random model. This difference in performance on the NonLinX dataset is due to the structural design of the NAM-based models CoxNAM and CoxSENAM.

In the cases of the real datasets, all models performed similarly on the FLCHAIN dataset except for the CPH model. More intriguingly, models show three levels of performance on the SEER dataset. The best performance is demonstrated

by CoxSE and DeepSurv with no significant difference between the two. On the other hand, CoxNAM and CoxSENAM also performed similarly, however, significantly lower than CoxSE and DeepSurv. Finally, CPH performed significantly lower than the four other models. Such results on the SEER dataset could indicate non-linearity and interaction between the features.

Model/Dataset	Lin	NonLin	NonLinX	FLCHAIN	SEER
CPH	67.67±0.020	(50.07±0.078)	(50.01±0.069)	(78.33±0.094)	(80.05±0.103)
DeepSurv	67.68±0.001	75.30±0.011	77.92±0.018	78.45±0.095	84.35±0.027
CoxNAM	67.67±0.011	75.30±0.012	(70.84±0.092)	78.59±0.169	(83.86±0.018)
CoxSENAM	67.67±0.012	75.31±0.006	(70.93±0.118)	78.51±0.057	(83.85±0.029)
CoxSE	67.68±0.001	75.29±0.024	77.93±0.021	78.57±0.031	84.37±0.018

Table 1: C-Index performance of all the models on all the datasets. The (.) indicates a significant difference.

5.3 Aggregated Explanations

The aggregated explanations are computed as the mean of the absolute values of explanations of the explained instances:

$$exp_i = \frac{1}{n} \sum_{j=0}^{n-1} |f_{exp}^i(\mathbf{x}_j)| \quad (21)$$

where $f_{exp}^i(\cdot)$ is the explanation value returned by the model of the feature of index i , \mathbf{x}_j is the features vector of the instance j , and n is the number of the explained instances.

Results illustrated in Figures 4, 5, and 6 show the aggregated explanations of the models on the three synthetic datasets sorted by their average effect. In general, most models agree with the ground truth of the generated data, however, a few intriguing cases deviate from it. Firstly, CoxNAM on the Lin dataset, illustrated in Figure 4d, ranked the features incorrectly although it achieved the same performance as the other models. This could suggest that modeling the output as an additive function, as in the NAM models, does not guarantee providing correct explanations. Moreover, it indicates the importance of the role of the regularization terms in the CoxSE and CoxSENAM models. It also signifies the proposal of the hybrid model CoxSENAM as a better-regularized version of the NAM-based models. Another case is the CoxNAM explanations on the NonLinX dataset where although it ranked the features correctly, their relative magnitudes are not comparable to the ground truth in contrast to the same-performing model CoxSENAM. Finally, although the CPH model ranked the features correctly on the NonLin dataset and incorrectly on the NonLinX dataset, both explanations can be considered random due to the model’s poor random performance ($\approx 50\%$ C-index) on these two non-linear datasets.

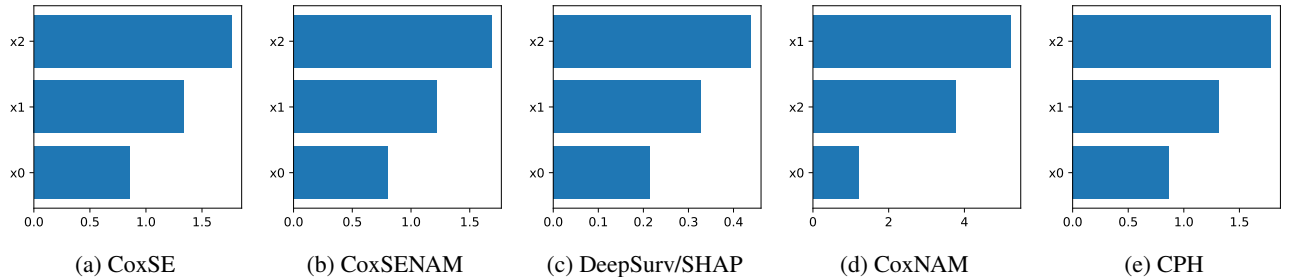


Figure 4: Lin Dataset Aggregated Explanations

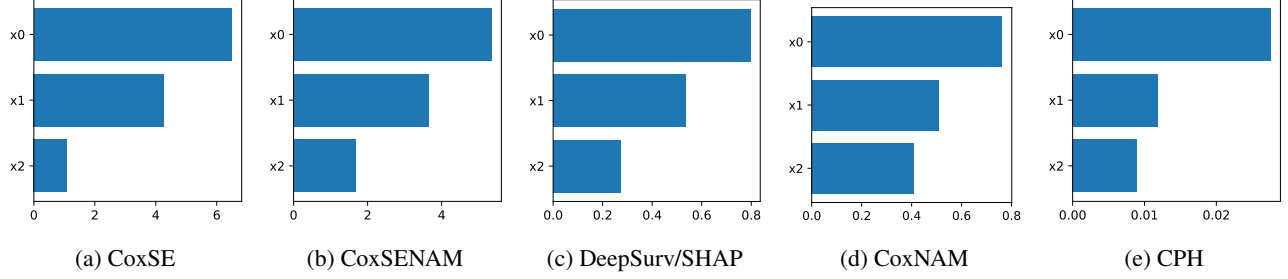


Figure 5: NonLin Dataset Aggregated Explanations

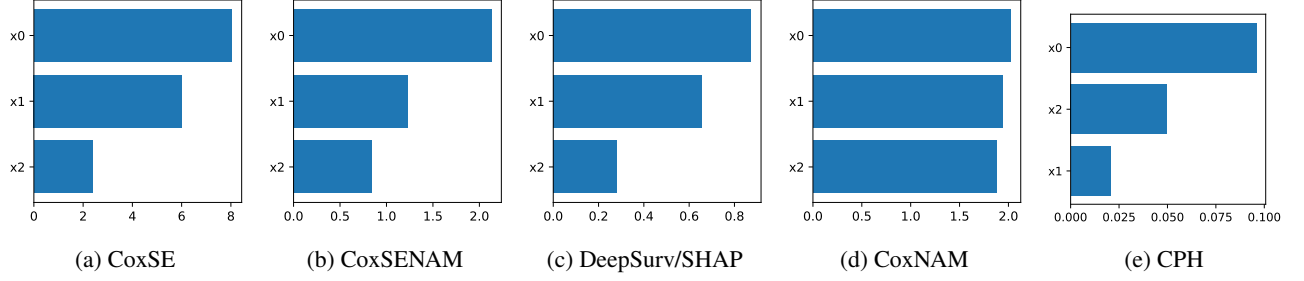


Figure 6: NonLinX Dataset Aggregated Explanations

5.4 Feature Interactions

In the previous section, the results on the NonLinX dataset showed a large discrepancy between DeepSurv and CoxSE on one side and the NAM-based models on the other side. The two NAM-based models, as they have a separate model for each feature, learn the contribution of each feature based only on its corresponding feature neglecting the interactions between the features. This is evident from the experimental results shown in Figure 7. In this experiment, we created seven synthetic datasets based on the log-risk function in Equation 22 with varying the interaction strength factor λ .

$$f(\mathbf{x}) = 3x_0^2 + x_1^2 + \lambda x_0 x_1 \tag{22}$$

DeepSurv model is the most flexible among the other Cox-based models as it holds no design assumptions on the function $f(\mathbf{x})$, other than that it is modeled as a feed-forward neural network. In contrast to DeepSurv, the other models, CPH, CoxSE, CoxNAM, and CoxSENAM force structural constraints making their hypothesis spaces subspaces of the DeepSurvs hypothesis space. Aside from fluctuations resulting from over or under-fitting, DeepSurv performance is guaranteed to be the upper bound for the rest of the Cox-based models. Figure 7 shows the deviation of the models' performance from DeepSurv performance. The NAM-based models' performance degrades with the increase of the interaction strength, while the CoxSE model maintains an equivalent performance to DeepSurv.

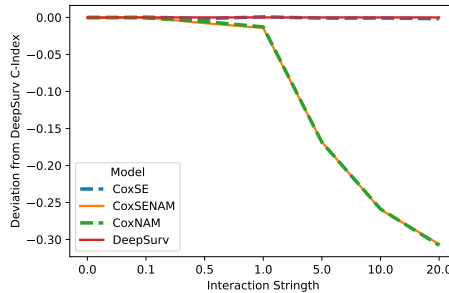


Figure 7: Feature interactions' effect on models' performance

5.5 Explanations Stability

The stability is assessed using the Lipschitz constant, Equation 23, which quantifies the model’s sensitivity to a small change in the input [8]. It estimates the maximum change in explanation for a small change in the vicinity of the point of interest.

$$L = \operatorname{argmax}_{x_j \in \epsilon(x_i)} \frac{\|f_{expl}(x_i) - f_{expl}(x_j)\|_2}{\|x_i - x_j\|_2} \tag{23}$$

where $\epsilon(x_i)$ is the neighborhood of x_i .

We use the sample-based Lipschitz estimation in Equation 23. In this regard, the $\epsilon(x_i)$ are the set of points in the neighborhood of x_i . Moreover, we used the angle between the explanations as a distance metric. This choice is due to the special nature of Cox Proportional Hazards models. In such models, the scale of the output values does not matter as long as they maintain the same order. Consequently, two models that are the same except for a scaling factor result in different stability values.

The results illustrated in Figures 8 show that the CPH model has the best stability. This is unsurprising as it is a linear model that has a global explanation for all points. Additionally, CoxSE and CoxSENAM models achieved better stability compared to CoxNAM and DeepSurv(+SHAP). This improvement can be attributed to the regularization term \mathcal{L}_2 weighted by α in their loss function. In CoxSE and CoxSENAM models, the \mathcal{L}_2 term controls the model’s flexibility locally. Higher α values result in less flexible models. In the limit, they converge to linear models for very high α values, i.e., the least flexibility and best stability.

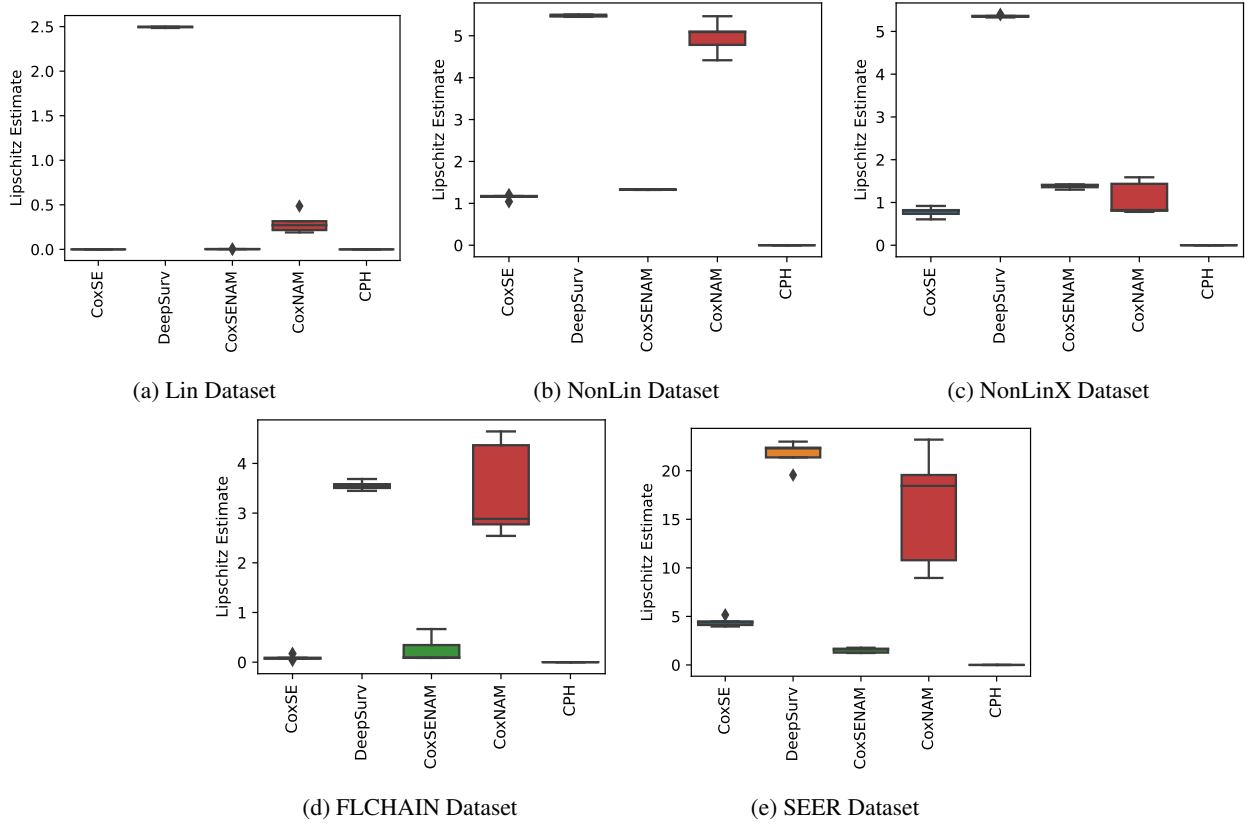


Figure 8: Comparison between the models’ stability across different datasets (lower is more stable)

5.6 Robustness to Non-informative Features

The robustness is computed as the ratio of the informative to the non-informative contributions of the features. The higher the ratio the more robust the model is to noisy features, in which case more contribution comes from informative

features relative to non-informative features.

$$Robustness = \sum_{i=0}^N \frac{y_i^\Omega}{y_i^{\overline{\Omega}}} \quad (24)$$

where:

$$y^\Omega = \sum_{x_i \in \Omega(\mathbf{x})} w_i(\mathbf{x})x_i \quad (25)$$

$$y^{\overline{\Omega}} = \sum_{x_i \in \overline{\Omega(\mathbf{x})}} w_i(\mathbf{x})x_i \quad (26)$$

where $\Omega(\mathbf{x})$ is the set of informative features of \mathbf{x} and $\overline{\Omega(\mathbf{x})}$ is its complement, i.e., the set of non-informative features.

In this experiment, to guarantee that the three models, CoxSE, CoxNAM, and CoxSENAM can model the data with comparable performances, we created synthetic datasets with non-linear log-risk as in Equation 22 without interaction ($\lambda = 0$) varying the dataset size from 1k to 50k samples. Each dataset contains 10 features, two of which are informative and the rest are non-informative features. To study the models' robustness and the effect of dataset size and the regularization parameters, we ran several experiments varying the dataset size and α and β for the CoxSE and the CoxSENAM models.

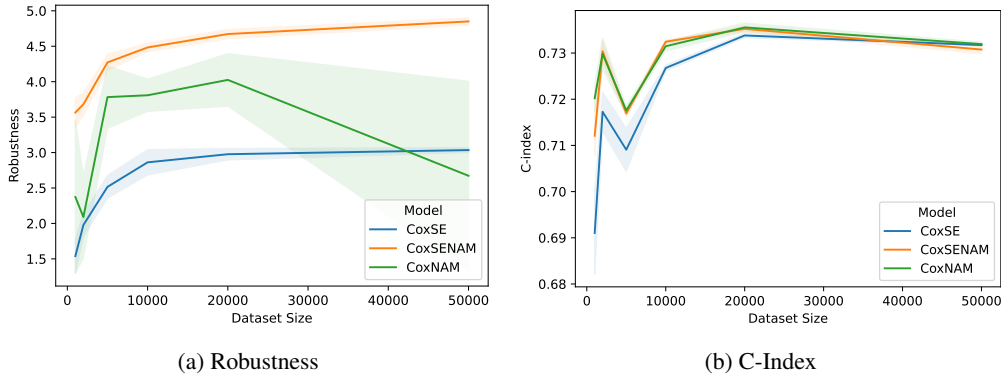


Figure 9: Comparison between the models' performance and robustness across different dataset sizes

The results in Figure 9 show that all models benefit from increasing the dataset size in improving the C-index, Figure 9b and models' robustness, Figure 9a. Moreover, for very small and very large dataset sizes, CoxSE and CoxNAM have a comparable robustness score. At the same time, CoxNAM Shows better robustness than CoxSE in med-size datasets as illustrated in Figure 9a. This can be attributed to the design structure of CoxNAM where non-informative features only contribute to the final decision in the neural network in the form of additive noise. In CoxSE, however, computing feature relevances incorporates all the informative and non-informative features passed through the neural network in a complicated way. This makes it harder for the CoxSE model to isolate the noise. However, the hybrid model, CoxSENAM demonstrated better robustness which can be attributed to the extra regularization term \mathcal{L}_3 weighted by β in its loss function. To illustrate that, Figure 10, shows the effect of dataset size and the change in β , the weight of the \mathcal{L}_3 term common for both CoxSE and CoxSENAM loss functions. Increasing β does not seem to have any effect on the CoxSE model's robustness, however, the effect is significant in the case of CoxSENAM as shown in Figures 10a and 10b respectively.

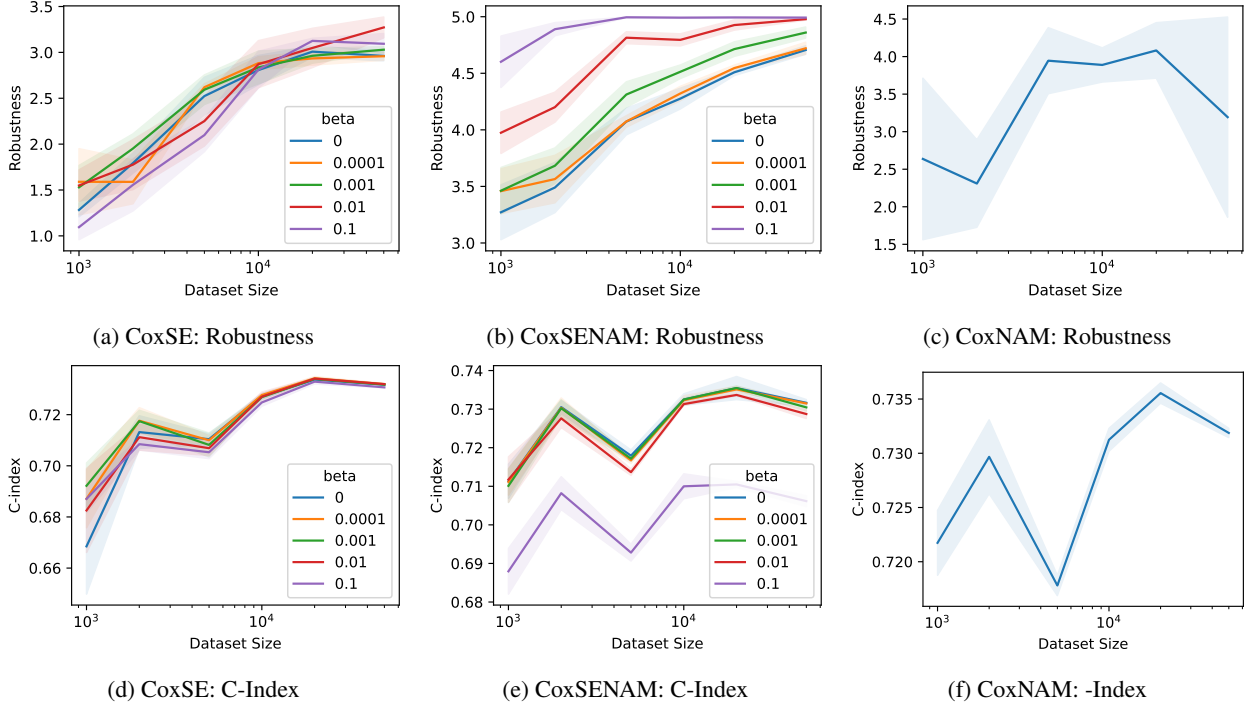


Figure 10: Comparison between the models' performance and robustness across different dataset sizes and different β values

6 Explanations Assessment on Real Datasets

In this section, we discuss the results of the two real datasets FLCHAIN and SEER. With the existence of co-linearities and correlations between the features, models can rely on different subsets of features which result in different explanations. However, as we do not know the ground truth of these datasets, an interesting validation method would be to compare how consistent the explanations provided by the model are with the explanations provided by an external method like SHAP applied to the model itself.

The SHAP method models the features' contribution to the model's decision. Whereas, CoxSE and CoxSENAM models produce explanations in terms of locally linear weights, which represent the sensitivity to change in the respective features. Based on such weights, we can compute the contribution in a similar way SHAP does for a linear model.

Given a linear model trained on a dataset with m features and has weights $\beta_i : i \in 0..m - 1$, the Shapley Values Φ_i of the feature x_i weighted by β_i can be written as:

$$\Phi_i = \beta_i(x_i - \mathbb{E}(x_i)) \tag{27}$$

Based on Equation 27, we compute the contributions of the features for the CoxSE and the CoxSENAM by replacing the constant weights with their variable weights as:

$$\Phi_i = w_i(\mathbf{x})(x_i - \mathbb{E}(x_i)) \tag{28}$$

We compared the rank order of the features provided by each model against the rank order of the SHAP explanation of the same model. We used the weighted- τ [31] which is a weighted version of Kendall- τ [32] rank correlation index. The weighted- τ penalizes the disagreement in the higher ranked items more than the lower ones. This makes it convenient for comparing feature ranking. Except for the approximation error of the SHAP method, the results in Figure 11 show almost a perfect correlation between the linear CPH model's explanations and its Shapley Values. This is understandable due to the direct relationship between Shapley Values and the linear weights as shown in Equation 27. The results also show a clear advantage of the SENN-based models (CoxSE and CoxSENAM) which have much higher correlations with their own Shapley Values than the CoxNAM model. This can be attributed to the local linearity of the models encouraged by the regularization term \mathcal{L}_2 .

It is worth noting that there was a complete match between the ranking of the aggregated explanations of all models with the ranking of their own aggregated Shapley Values except for the case of CoxNAM on the Lin dataset shown in

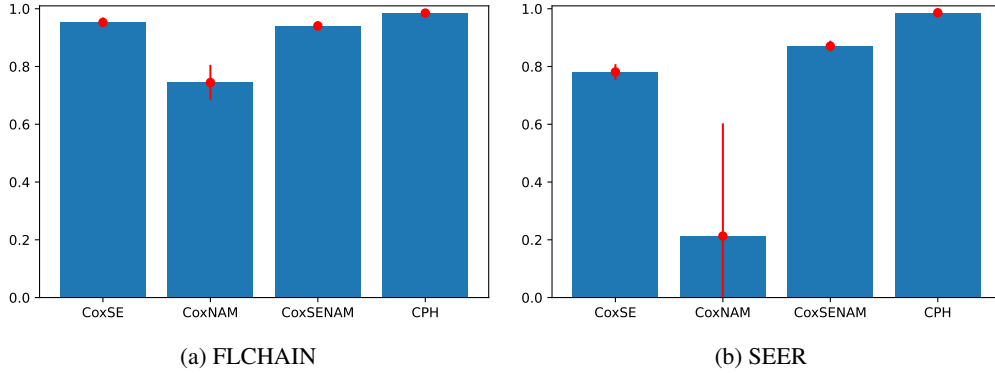


Figure 11: Rank correlation between the models' explanation and its own Shapley Values

Figure 4d. This can explain the lower correlation between CoxNAM and its SHAP explanations in the case of the real datasets. Moreover, this strengthens the hypothesis that transforming the function into an additive function does not guarantee valid explanations and highlights the importance of the regularization terms in the SENN-based models in the validity of the generated explanations.

7 Conclusion

In this work, we explored how self-explaining neural networks with the CPH model can be adapted for survival modeling. We proposed two CPH-based models, CoxSE relying on the SENN structure, and CoxSENAM which is a hybrid model between SENN and the NAM structures. The two models share the same type of output and loss function providing local explanations as a locally linear approximation of the underlying function. In this regard, unlike Shapley Values and the CoxNAM model which provide explanations as feature contributions, our models' explanations come in the form of local weights. As such, they highlight the sensitivity of the outcome to changes in the features in the vicinity of the point of interest. However, we illustrated that feature contributions can be computed directly from such weights similar to the case of a linear model, however, with variable weights.

We performed several experiments with synthetic and real datasets which highlighted the properties of the proposed models. In terms of performance, CoxSE was shown to be a flexible model that matches the performance of its black-box counterpart; DeepSurv. However, similar to the CoxNAM model, CoxSENAM is less flexible due to the NAM structure which cannot handle interactions between the features. Nevertheless, CoxSE and CoxSENAM showed better stability than CoxNAM and DeepSurv (explained by SHAP) and better matching with the ground truth than CoxNAM. This is due to the regularization term weighted by α in their loss function that directly encourages local similarity of explanations.

On the other hand, the NAM-based models showed better robustness to noisy features than the CoxSE model. This can be attributed to the structure of the NAM models where the noise contribution to the output comes as additive noise. This makes it easier for the NAM-based models to isolate the noise transforming it into a constant value added to the output. However, our hybrid model, CoxSENAM, showed better robustness than CoxNAM, assigning less importance to noisy features. This can be attributed to the second regularization term weighted by β encouraging the noise contribution to be close to zero.

Lastly, using real datasets, our models CoxSE and CoxSENAM demonstrated better consistency between their intrinsic explanations and the post-hoc explanation provided by SHAP. This was also observed on the synthetic datasets which arguably indicates the validity of such explanations in describing the underlying contributions of the features. On the other hand, CoxNAM demonstrated less consistency with its post-hoc explanations on both, the real and synthetic datasets.

A Hyperparameters Tuning

Five-fold cross-validation was used to tune the models' hyperparameters number of layers, number of nodes per layer, L_2 regularization weight, dropout rate, and learning rate. Moreover, we tuned α and β weights of the loss function for the CoxSE and CoxSENAM models. The selected hyperparameters are listed in Tables 2, 3, 4, 5, and 6.

Hyperparameter	CoxSE	CoxSE _{NAM}	DeepSurv	Cox _{NAM}	CPH
No. Layers	4	1	3	2	-
No. Nodes	128	4	4	32	-
L2	0	0.5	0.1	0.7	-
Dropout	0.4	0	0	0	-
Learning Rate	0.01	0.1	0.05	0.1	0.1
alpha	0.5	0.5	-	-	-
beta	0	0.005	-	-	-

Table 2: hyperparameters of the models on the Lin dataset

Hyperparameter	CoxSE	CoxSE _{NAM}	DeepSurv	Cox _{NAM}	CPH
No. Layers	1	1	1	4	-
No. Nodes	4	128	128	128	-
L2	0.5	1	0.01	1	-
Dropout	0	0.4	0	0	-
Learning Rate	0.001	0.006	0.001	0.0009	0.0003
alpha	3e-6	9e-6	-	-	-
beta	5e-4	9e-6	-	-	-

Table 3: hyperparameters of the models on the NonLin dataset

Hyperparameter	CoxSE	CoxSE _{NAM}	DeepSurv	Cox _{NAM}	CPH
No. Layers	1	1	1	2	-
No. Nodes	32	64	128	128	-
L2	0.5	0	0.5	0.05	-
Dropout	0	0.1	0	0	-
Learning Rate	0.1	0.1	0.0001	0.05	0.03
alpha	1e-5	3e-3	-	-	-
beta	1e-4	5e-6	-	-	-

Table 4: hyperparameters of the models on the NonLinX dataset

Hyperparameter	CoxSE	CoxSE _{NAM}	DeepSurv	Cox _{NAM}	CPH
No. Layers	4	4	1	4	-
No. Nodes	4	32	16	64	-
L2	0.5	0.001	1	0	-
Dropout	0.3	0.4	0.1	0	-
Learning Rate	0.01	0.003	0.0005	0.001	0.09
alpha	4e-5	6e-5	-	-	-
beta	6e-3	5e-5	-	-	-

Table 5: hyperparameters of the models on the FLCHAIN dataset

Hyperparameter	CoxSE	CoxSE _{NAM}	DeepSurv	Cox _{NAM}	CPH
No. Layers	1	4	1	4	-
No. Nodes	4	16	32	16	-
L2	0.5	0.5	1	0.05	-
Dropout	0	0	0.2	0	-
Learning Rate	0.0009	0.001	0.0005	0.0005	0.01
alpha	1e-5	7e-5	-	-	-
beta	3e-5	5e-6	-	-	-

Table 6: hyperparameters of the models on the SEER dataset

References

- [1] A. Alabdallah, M. Ohlsson, S. Pashami, T. Rögnavaldsson, The concordance index decomposition: A measure for a deeper understanding of survival prediction models, *Artificial Intelligence in Medicine* 148 (2024) 102781. doi:<https://doi.org/10.1016/j.artmed.2024.102781>.
- [2] M. Reza, M. Wirth, T. Tammela, V. Cicalese, F. G. Veiga, P. Mulders, K. Miller, A. Tubaro, F. Debruyne, A. Patel, C. Caris, W. Witjes, O. Thorsson, P. Wollmer, L. Edenbrandt, M. Ohlsson, E. Trägårdh, A. Bjartell, Automated bone scan index as an imaging biomarker to predict overall survival in the zometa european study/spcg11, *European Urology Oncology* 4 (1) (2021) 49–55. doi:[10.1016/j.euo.2019.05.002](https://doi.org/10.1016/j.euo.2019.05.002).
- [3] E. Polymeri, M. Sadik, R. Kaboteh, P. Borrelli, O. Enqvist, J. Ulén, M. Ohlsson, E. Trägårdh, M. H. Poulsen, J. A. Simonsen, P. F. Hoiland-Carlsen, Å. A. Johnsson, L. Edenbrandt, Deep learning-based quantification of pet/ct prostate gland uptake: association with overall survival, *Clinical Physiology and Functional Imaging* 40 (2) (2020) 106–113. doi:<https://doi.org/10.1111/cpf.12611>.
- [4] A. Alabdallah, T. Rögnavaldsson, Y. Fan, S. Pashami, M. Ohlsson, Discovering premature replacements in predictive maintenance time-to-event data, *Proceedings of the Asia Pacific Conference of the PHM Society 2023* 4 (1) (2023). doi:[10.36001/phmap.2023.v4i1.3609](https://doi.org/10.36001/phmap.2023.v4i1.3609).
- [5] M. Rahat, Z. Kharazian, P. Sheikholharam Mashhadi, T. Rögnavaldsson, S. Choudhury, Bridging the gap: A comparative analysis of regressive remaining useful life prediction and survival analysis methods for predictive maintenance, *PHM Society Asia-Pacific Conference* 4 (1) (Sep. 2023). doi:[10.36001/phmap.2023.v4i1.3646](https://doi.org/10.36001/phmap.2023.v4i1.3646).
- [6] S. Pashami, S. Nowaczyk, Y. Fan, J. Jakubowski, N. Paiva, N. Davari, S. Bobek, S. Jamshidi, H. Sarmadi, A. Alabdallah, R. P. Ribeiro, B. Veloso, M. Sayed-Mouchaweh, L. Rajaoarisoa, G. J. Nalepa, J. Gama, Explainable predictive maintenance, *arXiv (preprint)* (2023). doi:[10.48550/arXiv.2306.05120](https://doi.org/10.48550/arXiv.2306.05120).
- [7] R. Agarwal, L. Melnick, N. Frosst, X. Zhang, B. Lengerich, R. Caruana, G. E. Hinton, Neural additive models: Interpretable machine learning with neural nets, *Advances in neural information processing systems* 34 (2021) 4699–4711.
- [8] D. Alvarez Melis, T. Jaakkola, Towards robust interpretability with self-explaining neural networks, in: S. Bengio, H. Wallach, H. Larochelle, K. Grauman, N. Cesa-Bianchi, R. Garnett (Eds.), *Advances in Neural Information Processing Systems*, Vol. 31, Curran Associates, Inc., 2018.
- [9] L. V. Utkin, E. D. Satyukov, A. V. Konstantinov, Survnam: The machine learning survival model explanation, *Neural Networks* 147 (2022) 81–102. doi:<https://doi.org/10.1016/j.neunet.2021.12.015>.
- [10] L. Xu, C. Guo, Coxnam: An interpretable deep survival analysis model, *Expert Systems with Applications* 227 (2023) 120218. doi:<https://doi.org/10.1016/j.eswa.2023.120218>.
- [11] E. L. Kaplan, P. Meier, Nonparametric estimation from incomplete observations, *Journal of the American Statistical Association* 53 (282) (1958) 457–481. URL <http://www.jstor.org/stable/2281868>
- [12] W. Nelson, Hazard plotting for incomplete failure data, *Journal of Quality Technology* 1 (1) (1969) 27–52. doi:[10.1080/00224065.1969.11980344](https://doi.org/10.1080/00224065.1969.11980344).
- [13] W. Nelson, Theory and applications of hazard plotting for censored failure data, *Technometrics* 14 (4) (1972) 945–966. doi:[10.1080/00401706.1972.10488991](https://doi.org/10.1080/00401706.1972.10488991).
- [14] O. Aalen, Nonparametric Inference for a Family of Counting Processes, *The Annals of Statistics* 6 (4) (1978) 701–726. doi:[10.1214/aos/1176344247](https://doi.org/10.1214/aos/1176344247). URL <https://doi.org/10.1214/aos/1176344247>
- [15] D. R. Cox, Regression models and life-tables, *Journal of the Royal Statistical Society. Series B (Methodological)* 34 (2) (1972) 187–220. URL <http://www.jstor.org/stable/2985181>
- [16] J. L. Katzman, U. Shaham, A. Cloninger, J. Bates, T. Jiang, Y. Kluger, DeepSurv: personalized treatment recommender system using a cox proportional hazards deep neural network., *BMC medical research methodology* 18 (1) (2018) 24. doi:[10.1186/s12874-018-0482-1](https://doi.org/10.1186/s12874-018-0482-1).
- [17] C. Lee, W. Zame, J. Yoon, M. van der Schaar, Deephit: A deep learning approach to survival analysis with competing risks, *Proceedings of the AAAI Conference on Artificial Intelligence* 32 (1) (Apr. 2018). URL <https://ojs.aaai.org/index.php/AAAI/article/view/11842>

- [18] M. G. Altarabichi, A. Alabdallah, S. Pashami, M. Ohlsson, T. Rögnavaldsson, S. Nowaczyk, Improving concordance index in regression-based survival analysis: Discovery of loss function for neural networks, in: Proceedings of the Genetic and Evolutionary Computation Conference (GECCO), 2024. doi:10.1145/3638530.3664129.
- [19] S. Wiegrebe, P. Kopper, R. Sonabend, B. Bischl, A. Bender, Deep learning for survival analysis: a review, *Artificial Intelligence Review* 57 (3) (2024) 65. doi:10.1007/s10462-023-10681-3.
URL <https://doi.org/10.1007/s10462-023-10681-3>
- [20] F. E. Harrell Jr., R. M. Califf, D. B. Pryor, K. L. Lee, R. A. Rosati, Evaluating the Yield of Medical Tests, *JAMA* 247 (18) (1982) 2543–2546.
URL <https://doi.org/10.1001/jama.1982.03320430047030>
- [21] M. T. Ribeiro, S. Singh, C. Guestrin, "why should i trust you?": Explaining the predictions of any classifier, in: Proceedings of the 22nd ACM SIGKDD International Conference on Knowledge Discovery and Data Mining, KDD '16, Association for Computing Machinery, New York, NY, USA, 2016, p. 1135–1144. doi:10.1145/2939672.2939778.
URL <https://doi.org/10.1145/2939672.2939778>
- [22] S. M. Lundberg, S.-I. Lee, A unified approach to interpreting model predictions, in: I. Guyon, U. V. Luxburg, S. Bengio, H. Wallach, R. Fergus, S. Vishwanathan, R. Garnett (Eds.), *Advances in Neural Information Processing Systems*, Vol. 30, Curran Associates, Inc., 2017.
- [23] M. S. Kovalev, L. V. Utkin, E. M. Kasimov, Survlime: A method for explaining machine learning survival models, *Knowledge-Based Systems* 203 (2020) 106164. doi:<https://doi.org/10.1016/j.knosys.2020.106164>.
- [24] A. Alabdallah, S. Pashami, T. Rögnavaldsson, M. Ohlsson, Survshap: A proxy-based algorithm for explaining survival models with shap, in: 2022 IEEE 9th International Conference on Data Science and Advanced Analytics (DSAA), 2022, pp. 1–10. doi:10.1109/DSAA54385.2022.10032392.
- [25] M. Krzyżiński, M. Spytek, H. Baniecki, P. Biecek, Survshap(t): Time-dependent explanations of machine learning survival models, *Knowledge-Based Systems* 262 (2023) 110234. doi:<https://doi.org/10.1016/j.knosys.2022.110234>.
- [26] M. Kovalev, L. Utkin, F. Coolen, A. Konstantinov, Counterfactual explanation of machine learning survival models, *Informatica* 32 (4) (2021) 817–847. doi:10.15388/21-INF0R468.
- [27] A. Alabdallah, J. Jakubowski, S. Pashami, S. Bobek, M. Ohlsson, T. Rögnavaldsson, G. J. Nalepa, Understanding survival models through counterfactual explanations, in: *Computational Science – ICCS 2024*, Springer Nature Switzerland, Cham, 2024, pp. 310–324. doi:10.1007/978-3-031-63772-8_28.
- [28] T. Hastie, R. Tibshirani, Generalized additive models, *Statistical Science* 1 (3) (1986) 297–310.
URL <http://www.jstor.org/stable/2245459>
- [29] A. Dispenzieri, J. A. Katzmann, R. A. Kyle, D. R. Larson, T. M. Therneau, C. L. Colby, R. J. Clark, B. Graham P. Mead, S. Kumar, L. J. M. III, S. V. Rajkumar, Use of nonclonal serum immunoglobulin free light chains to predict overall survival in the general population., *Mayo Clin Proc.* 87 (6) (2012) 517–23.
URL <https://doi.org/10.1016/j.mayocp.2012.03.009>
- [30] M. A. Duggan, W. F. Anderson, S. Altekruse, L. Penberthy, M. E. Sherman, The surveillance, epidemiology, and end results (seer) program and pathology: Toward strengthening the critical relationship, *The American Journal of Surgical Pathology* 40 (12) (2016).
- [31] S. Vigna, A weighted correlation index for rankings with ties, in: Proceedings of the 24th International Conference on World Wide Web, WWW '15, International World Wide Web Conferences Steering Committee, Republic and Canton of Geneva, CHE, 2015, p. 1166–1176. doi:10.1145/2736277.2741088.
URL <https://doi.org/10.1145/2736277.2741088>
- [32] M. G. Kendall, A new measure of rank correlation, *Biometrika* 30 (1/2) (1938) 81–93.
URL <http://www.jstor.org/stable/2332226>